Supplementary Material

Specific conformational states of Ras GTPase upon effector binding

Julie Baussand* and Jens Kleinjung

Division of Mathematical Biology, MRC National Institute for Medical Research, The Ridgeway, Mill Hill, London NW7 1AA, United Kingdom

E-mail: jbaussa@nimr.mrc.ac.uk

Figure Legends

Figure S1 Sampling width and conformational change. Illustration of the selection method for fragments with significant differences in sampling width and conformational states between two systems. Comparison of three exemplary fragments *a* (A), *b* (B) and *c* (C) of $\text{Ras}^{PLC\varepsilon}$ and $\text{Ras}^{PI3K\gamma}$. (A) The conformational sampling of both systems is narrow, leading to a small ΔCS and large CD. The conformational distance is therefore dominated by the *CD* value. This example illustrates a true conformational change. (B) The conformational sampling of both systems is wide, leading to small ΔCS and CD values. A conformational change cannot be inferred for fragment *b*. (C) The conformational sampling of $\text{Ras}^{PI3K\gamma}$ is wide while the one of $\text{Ras}^{PLC\varepsilon}$ is narrow, the *CD* value is dominated by (and equal to) the large ΔCS. A conformational change cannot be inferred for fragment *c*. (D) The *CD versus* ΔCS plot captures the true conformational change of fragment *a* as

*To whom correspondence should be addressed

off-diagonal point, while fragments *c* lies on the diagonal $CD = \Delta CS$ (dashed grey line) and *b* lies just above with a low *CD* value. Solid grey lines show the 0.2 thresholds.

Figure S2 Contact maps. A. Map of persistent intramolecular contacts in Ras. Of the 755 persistent inter-residue contacts of Ras present in at least one system, 585 (77%) were present in all systems, 661 in $\text{Ras}^{PI3K\gamma}$, 678 in Ras^{Byr2}, 669 in Ras^{RalGDS} and 713 in $\text{Ras}^{PLC\varepsilon}$. Upper triangle: Inter-residue contact pairs present in *all* systems ($\times$), only in Ras^{B} systems ($\square$) and only in Ras^{U} systems ($\triangle$) are shown. Lower triangle: Specific inter-residue contact pairs; the different systems are colour coded. Grey dotted lines separate lobe1 and lobe2. B: Grey-scale plot of the interactions between Ras and effectors, plotted along the interface sequence of Ras.

Figure S3 Conformations and interactions at Y40. Structural comparison of the equivalent $\beta 2$ residues of (A) non-RA domain type effectors PI3Kγ and Byr2 (B) RA domain type effectors PLCε and RalGDS, which participate in Ras binding through interaction with Ras–S39 and Y40 (first and second rows). Bottom: Relative backbone torsion of effector $\beta 2$ induced by the different binding modes of non-RA and RA domains. The backbone of $\beta 2$ is curved in RA domains allowing PLCε–Q18 and RalGDS–N29 to interact with Ras–Y40. The backbone of $\beta 2$ is straight in non-RA domains where PI3Kγ–Q231 and Byr2–R83 interacts with Ras–Y40 while PI3Kγ–T228 and Byr2–G80 (equivalent to RA domains residues PLCε–Q18 and RalGDS–N29) are distant from Ras–40.

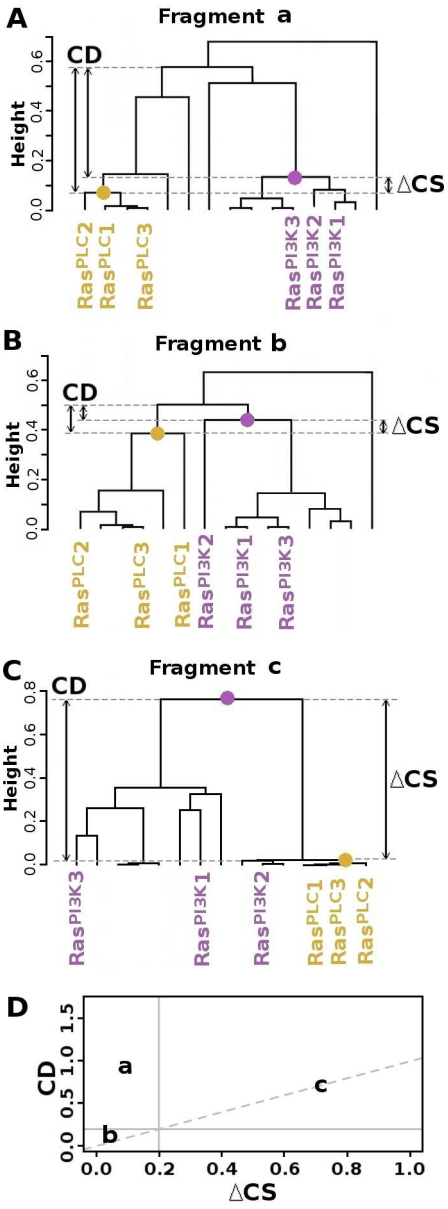
A
Fragment a
CD
ΔCS
Height
0.0
0.2
0.4
0.6
RasPLC2
RasPLC1
RasPLC3
RasPI3K3
RasPI3K2
RasPI3K1
B
Fragment b
CD
ΔCS
Height
RasPLC2
RasPLC3
RasPLC1
RasPI3K2
RasPI3K1
RasPI3K3
C
Fragment c
CD
ΔCS
Height
0.0
0.2
0.4
0.6
0.8
RasPI3K3
RasPI3K1
RasPI3K2
RasPLC1
RasPLC3
RasPLC2
D
CD
ΔCS
a
b
c
0.0
0.5
1.0
1.5
0.0
0.2
0.4
0.6
0.8
1.0

Figure S1:

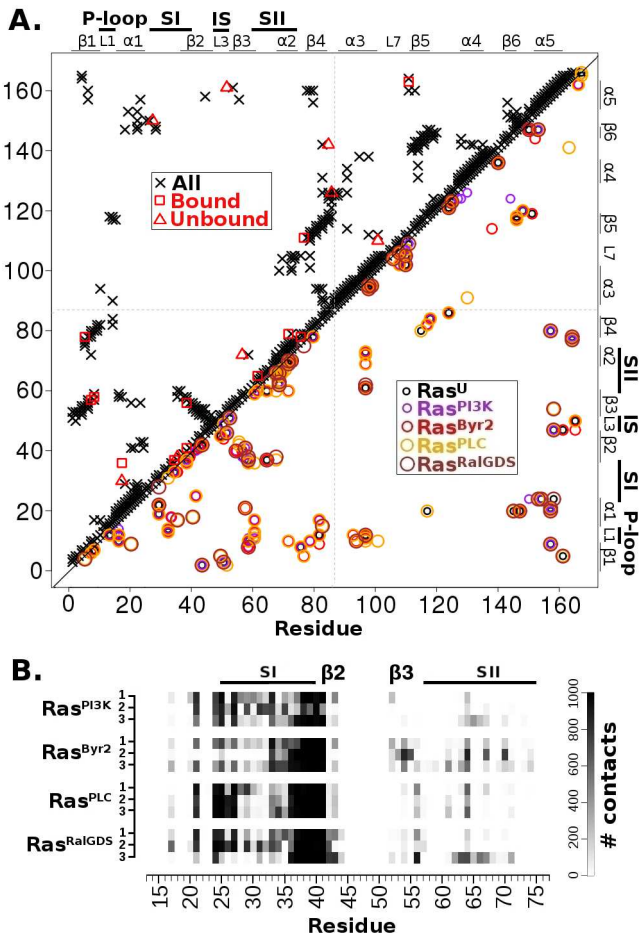
A.
P-loop
SI
IS
SII
β1 L1 α1 β2 L3 β3 α2 β4 α3 L7 β5 α4 β6 α5
All
Bound
Unbound
RasU
RasPI3K
RasByr2
RasPLC
RasRalGDS
Residue
B.
SI
β2
β3
SII
RasPI3K
RasByr2
RasPLC
RasRalGDS
contacts
Residue

Figure S2:

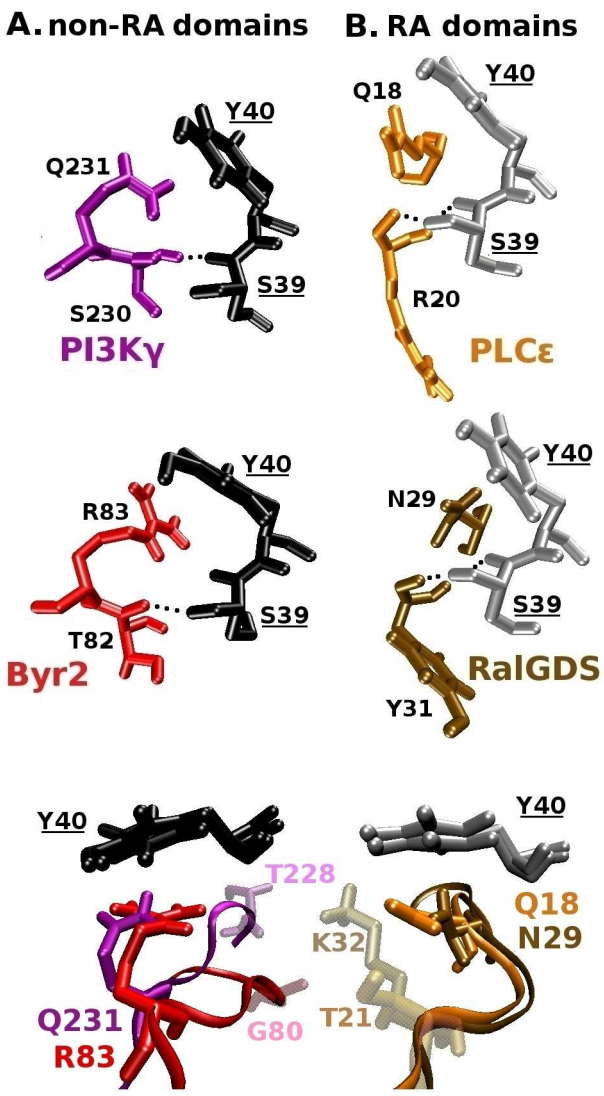
A. non-RA domains
B. RA domains
Y40
Q231
S39
S230
PI3Kγ
Q18
Y40
S39
R20
PLCε
Y40
R83
S39
T82
Byr2
Y40
N29
S39
RalGDS
Y31
Y40
T228
Q231
R83
G80
Y40
Q18
N29
K32
T21

Figure S3:

Table S1: Average and maximum (in parentheses) RMSD values in Å of the Ras backbone using the average structure of each trajectory as reference. RMSD was computed for each simulation replicate of each system as well as for the cumulative replicates (rep. all) and the concatenated system simulations (all systems).

	rep1	rep2	rep3	rep all
Ras^{U}	0.8 (1.4)	0.9 (2.1)	1.0 (2.1)	1.1 (2.2)
$Ras^{PI3K\gamma}$	1.3 (2.2)	0.9 (1.8)	1.0 (1.8)	1.3 (2.5)
Ras^{Byr2}	0.9 (1.8)	0.8 (1.4)	1.0 (1.6)	1.0 (1.9)
$Ras^{PLC\varepsilon}$	0.9 (1.8)	0.8 (1.6)	0.8 (1.9)	0.8 (1.9)
Ras^{RalGDS}	1.0 (1.9)	0.8 (1.6)	0.9 (1.8)	1.1 (2.0)
all systems				1.3 (2.7)

Table S2: Average distance and standard deviation (Å) between pairs of residues in Ras^{U}, $Ras^{PI3K\gamma}$, Ras^{Byr2}, $Ras^{PLC\varepsilon}$ and Ras^{RalGDS}. Pairs of residues corresponding to persistent inter-residue contact pairs in a system are indicated in bold.

	Ras^{U}	$Ras^{PI3K\gamma}$	Ras^{Byr2}	$Ras^{PLC\varepsilon}$	Ras^{RalGDS}
Ras^{U}					
17-29	**3.9±0.5**	4.2±0.8	4.1±0.7	4.2±0.5	5.3±1.0
27-149	**3.9±0.7**	4.3±0.8	4.0±0.8	3.9±0.7	4.7±1.0
35-37	**3.7±0.3**	4.0±0.3	3.7±0.5	4.0±0.3	4.2±0.3
51-160	**3.9±0.7**	4.3±1.0	5.2±1.5	4.0±0.7	4.1±0.8
56-71	**3.5±1.0**	4.3±0.9	5.0±0.8	4.1±0.5	4.0±0.6
84-141	**3.8±0.6**	4.7±0.7	4.0±0.7	4.0±0.7	4.3±0.7
85-125	**4.0±0.3**	4.1±0.3	4.0±0.3	4.0±0.3	4.0±0.3
100-109	**4.0±0.4**	4.1±0.4	4.0±0.6	4.1±0.4	4.2±0.5
Ras^{B}					
5-77	3.0±1.2	**2.2±0.4**	**2.2±0.3**	**2.1±0.3**	**2.1±0.3**

	Ras^{U}	$Ras^{PI3K\gamma}$	Ras^{Byr2}	$Ras^{PLC\varepsilon}$	Ras^{RalGDS}
7-56	4.0±0.6	**3.6±0.2**	**3.6±0.2**	**3.5±0.2**	**3.5±0.2**
8-57	4.1±0.6	**3.8±0.3**	**3.9±0.3**	**3.8±0.3**	**3.7±0.3**
17-35	4.3±1.5	**2.8±0.1**	**2.8±0.1**	**2.4±0.2**	**2.9±0.7**
34-36	4.2±0.5	**3.8±0.4**	**3.7±0.4**	**3.8±0.4**	**3.6±0.4**
38-40	3.2±1.0	**3.0±0.6**	**2.2±0.5**	**2.8±0.5**	**3.0±0.4**
38-55	3.8±0.4	**3.4±0.4**	**3.2±0.4**	**3.8±0.4**	**3.8±0.3**
61-64	3.0±1.1	**2.8±1.0**	**2.4±0.5**	**2.5±0.7**	**2.5±0.5**
71-78	3.4±0.8	**2.9±0.5**	**2.9±0.5**	**2.9±0.5**	**2.9±0.6**
75-77	3.9±0.5	**3.6±0.4**	**3.6±0.4**	**3.7±0.4**	**3.6±0.3**
76-110	3.9±0.6	**3.6±0.4**	**3.6±0.4**	**3.5±0.4**	**3.5±0.4**
110-162	4.3±0.9	**3.9±0.5**	**3.9±0.5**	**3.9±0.5**	**3.9±0.5**
$Ras^{PI3K\gamma}$					
10-58	3.8±0.8	**3.8±0.5**	4.2±0.7	4.3±0.8	3.6±1.2
13-16	3.9±0.4	**3.8±0.4**	4.3±0.6	4.1±0.4	4.7±0.8
23-149	4.2±1.1	**3.8±1.1**	4.3±1.3	4.1±1.2	4.1±1.1
123-126	5.0±0.9	**4.0±1.0**	4.8±1.0	4.8±1.0	4.3±1.1
123-127	4.6±1.2	**3.6±1.3**	4.4±1.2	4.5±1.4	3.9±1.3
123-143	5.2±1.8	**3.8±1.9**	5.0±1.8	4.8±1.9	4.3±2.0
125-129	4.7±1.2	**4.0±1.0**	4.6±1.1	4.7±1.2	4.4±1.1
Ras^{Byr2}					
8-81	4.0±0.3	4.0± 0.3	**3.8±0.3**	4.1±0.4	4.0±0.4
43-50	4.5±1.6	4.5± 1.6	**4.0±1.5**	5.7±1.4	5.3±1.6
46-164	4.6±1.8	5.5± 2.3	**3.4±0.8**	5.2±2.2	6.1±2.2
113-137	4.3±1.1	5.0± 1.5	**4.0±0.8**	4.1±0.8	4.2±0.9

	Ras^{U}	$Ras^{PI3K\gamma}$	Ras^{Byr2}	$Ras^{PLC\varepsilon}$	Ras^{RalGDS}
143-151	4.2±0.6	4.2± 0.6	**4.0±0.6**	4.3±0.6	4.3±0.6
$Ras^{PLC\varepsilon}$					
1-51	4.5±0.9	4.4±0.9	4.4±0.9	**3.9±0.9**	4.1±0.9
9-96	3.7±0.7	3.7±0.7	3.9±0.7	**3.9±0.6**	3.9±0.7
9-100	4.0±0.3	4.9±1.1	4.1±0.4	**4.0±0.3**	4.2±0.4
11-60	4.3±0.9	4.0±0.5	4.4±1.0	**3.8±0.5**	5.0±1.2
30-32	4.0±0.6	4.0±0.6	4.0±0.5	**3.9±0.5**	3.8±1.0
35-60	5.0±1.6	4.8±0.8	4.1±1.0	**3.4±0.6**	5.4±0.8
36-67	4.0±0.8	5.3±1.5	4.6±1.5	**4.0±1.0**	4.9±2.0
41-55	4.0±0.3	3.9±0.6	4.0±0.3	**3.9±0.2**	4.0±0.2
42-55	4.2±0.4	4.2±0.5	3.9±0.5	**3.8±0.5**	4.0±0.5
59-67	4.0±1.0	4.6±1.7	4.4±1.0	**4.0±1.0**	5.6±2.4
66-69	3.7±0.8	4.8±1.3	3.7±1.1	**3.2±0.5**	3.6±1.0
66-70	3.2±1.3	4.1±1.6	3.6±2.0	**2.3±0.6**	3.0±1.4
90-129	4.0±1.0	3.5±1.1	4.0±1.0	**3.8±0.8**	3.8±1.0
140-162	5.0±1.5	4.3±0.8	4.3±0.8	**4.0±0.5**	4.3±1.0
Ras^{RalGDS}					
27-29	3.9±0.5	3.8±0.6	4.0±0.5	4.0±0.5	**3.7±0.5**
37-58	4.5±0.5	4.5±0.5	4.1±0.7	4.9±0.5	**3.9±0.5**
37-67	4.3±1.0	5.1±1.4	4.7±1.5	4.2±0.9	**3.7±0.9**
61-96	3.9±1.2	4.9±1.9	5.0±1.5	4.6±1.0	**3.1±0.8**
62-65	4.8±1.3	5.1±1.6	4.0±1.4	4.1±1.2	**3.5±0.9**
74-76	4.1±0.5	4.0±0.5	4.1±0.6	4.3±0.5	**3.9±0.5**